

Traffic Congestion Control using Distributed Extremum Seeking and Filtered Feedback Linearization Control Approaches

Pouria Karimi Shahri¹, Baisravan HomChaudhuri², Srinivas S. Pulugurtha³, Ali Mesbah⁴ and Amir H. Ghasemi¹

Abstract—This paper presents a hierarchical infrastructure-based control algorithm to manage mainstream traffic flow on freeways. At the upper level, a distributed Extremum-Seeking control approach is employed to determine the optimal density of vehicles in a congested cell. The local objective function is defined such that the average flow within the target cell is maximized to resolve the congestion, and the flow difference with its upstream cell is minimized to prevent back-propagating the congestion. At the lower level, a distributed Filtered Feedback Linearization controller is used to update the suggested velocity communicated to the vehicles so that the desired density determined by the upper level can be achieved in each cell. We adopted the METANET model to describe the aggregated dynamics of the traffic network. We tested the performance of these controllers via a MATLAB-VISSIM COM interface. The results demonstrate that the designed distributed controllers can achieve the desired closed-loop performance despite unknown disturbances in an uncertain large-scale traffic network.

I. INTRODUCTION

The average American driver lost 36 hours (almost a week of work) due to traffic congestion in 2021 [1]. While building additional infrastructure may not be practically sustainable, various infrastructure-based and vehicle-based traffic control strategies have been developed to reduce the congestion [2].

The infrastructure-based algorithms, using the macroscopic models of a traffic network, focus on improving the aggregated traffic behavior (such as overall traffic flow) [3]. Infrastructure-based controllers include ramp-metering, variable speed limit (VSL) control, and lane management [4]. The main challenges associated with the design of infrastructure-based traffic controllers are due to (i) uncertainty and nonlinearity of the traffic system macroscopic dynamics and (ii) significant computational load of centralized macro-level controllers [5]. For instance, METNAET

traffic model [6] describes the traffic dynamics in terms of the density and average velocity of the vehicles within a traffic network. However, the model parameters of the METANET model are state-dependent and, thus, hard to characterize. Furthermore, the optimal operating density of a congested cell with an unknown downstream bottleneck is not known perfectly. To address these issues, different algorithms, including model-free based control algorithms, have been investigated [7]. In [8], Extremum Seeking (ES) control is employed for traffic congestion control with a downstream bottleneck. In this study, an unknown flow-density relationship is considered at the bottleneck area, and the optimum density of the upstream cell is determined to mitigate the congestion. Moreover, they assumed the traffic flow to be the control input; however, direct traffic flow control is not practical. To address this issue, a set-point tracking controller shall be integrated into the design of an ES-based controller [9]. An example of a set-point tracking controller that has been widely used for traffic control is the Feedback Linearization (FL) approach. The advantage of this method is its strength in addressing the challenges caused by the non-linearity in the macroscopic dynamics [10]. However, the main drawback of FL is that it requires model information. Because the traffic dynamics contain uncertainties associated with the unmodeled dynamics of a traffic system, which can intrinsically be state- and control-dependent, making it impractical to get the required model information for the FL controller. This paper addresses this shortcoming by introducing the Distributed Filtered Feedback Linearization (D-FFL) approach. D-FFL is a high-parameter-stabilizing control technique that addresses both command following and disturbance rejection for Multi-Input-Multi-Output (MIMO) nonlinear systems where the equilibrium of the zero dynamics is locally asymptotically stable [11]. D-FFL is mathematically equivalent to low-pass filtering, a standard feedback linearization controller. However, unlike the standard FL, the controller only requires limited model information, specifically, knowledge of the vector relative degree and the dynamic-inversion matrix. As a result, d-FFL makes the \mathcal{L}_∞ of the command following error arbitrarily small despite the presence of unknown disturbances [12].

This paper presents a distributed hierarchical control framework to leverage the advantages of both ES and FFL controllers, with ES at the upper level and FFL at the lower level. We discretize a freeway into multiple cells. We

*This work was not supported by any organization

¹Pouria Karimi Shahri is a Ph.D. Candidate in the Department of Mechanical Engineering, University of North Carolina at Charlotte, Charlotte, NC, USA Pkirimis@uncc.edu

²Baisravan Homechduri is with the Faculty of the Department of Mechanical Engineering, Illinois Institute of Technology, Chicago, IL, USA bhomchaudhuri@iit.edu

³Srinivas S. Pulugurtha is with the Faculty of the Department of Civil and Environmental Engineering, University of North Carolina at Charlotte, Charlotte, NC, USA sspulugurtha@uncc.edu

⁴Ali Mesbah is with the Faculty of the Department of Chemical and Biomolecular Engineering, University of California Berkeley, Berkeley, CA, USA mesbah@berkeley.edu

¹Amir H. Ghasemi is with the Faculty of the Department of Mechanical Engineering, University of North Carolina at Charlotte, Charlotte, NC, USA ah.Ghasemi@uncc.edu

adopt the METNAET model [6] to describe the macroscopic dynamics of each cell. At the upper level, we employ a distributed ES algorithm to find the optimal density of the congested cell to maximize the average flow of the target cell and minimize its flow difference with the upstream cell. Furthermore, we use distributed FFL controller to ensure each cell reaches its desired density by controlling the average velocity of the vehicles within the cell and its upstream cell. The contributions of this paper can be summarized as follows:

- Designing a scalable hierarchical infrastructure-based traffic controller (D-ES-FFL) that requires only limited traffic model information and is robust to an unknown disturbance in the traffic system.
- Establishing a MATLAB-VISSIM COM interface that allows closed-loop control of a simulated traffic scenario in PTV-VISSIM and validating the effectiveness of the distributed ES-FFL control approach using this interface.

The outline of this paper is as follows. Section II presents the basics of the homogeneous METNAET model for describing the macroscopic dynamics of a freeway traffic system. Section III discusses the design of the hierarchical control approach to achieve the desired traffic behavior. Section IV presents the simulation results, which show the effectiveness of the D-ES-FFL control approach for managing a freeway traffic system. Finally, Section V consists of this research's conclusions and future directions.

II. MACROSCOPIC DYNAMICS OF A FREEWAY

Consider a freeway traffic network, as shown in Fig. 1, wherein the road is discretized into multiple cells. We characterize cell, \mathcal{C}_i , where $i \in \{1, 2, \dots, n\}$, by the density of vehicles (ρ_i), space mean speed of vehicles (v_i) within the cell, and the total average flow rate (q_i) of the cell. We adopt a METANET model wherein the traffic states are the density and average velocity of vehicles in a cell to determine the macroscopic dynamics of the freeway network. Specifically, the dynamics of cell \mathcal{C}_i are described by

$$\dot{\rho}_i(t) = \frac{1}{L_i \lambda_i} (q_{i-1}(t) - q_i(t) + d_{i,\rho}(t)) \quad (1a)$$

$$\dot{v}_i(t) = \frac{1}{\tau_i} (U_i(t) - v_i(t)) + \frac{1}{L_i} \left[v_i(t) (v_{i-1}(t) - v_i(t)) - \frac{\varepsilon_i}{\tau_i} \frac{\rho_{i+1}(t) - \rho_i(t)}{\rho_i(t) + \kappa_i} \right] \quad (1b)$$

$$q_i(t) = \rho_i(t) v_i(t), \quad (1c)$$

where $d_{i,\rho}(t)$ is a disturbance (e.g., uncontrolled traffic demand including the off-ramps and on-ramps), λ_i is the number of the lanes in each cell, and L_i is the length of each cell. Here, $U_i(t) = (1 - \beta_i(t)) V_i(t)$ is considered the suggested velocity for the vehicles in the traffic network, where $V_i(t) = v_{\text{FF}} \exp \left[\frac{-1}{a_{m,i}} \left(\frac{\rho_i(t)}{\rho_c} \right)^{a_{m,i}} \right]$ is the steady-state velocity-density relationship in the Macroscopic Fundamental Diagram (MFD) [13]. v_{FF} is the free-flow velocity, and

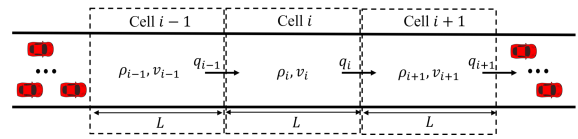


Fig. 1: Schematic of a traffic network.

ρ_c is the critical density of a cell. Also, $a_{m,i}$, κ_i , τ_i and, ε_i are state-dependent model parameters for each cell. For the sake of simplicity, the model parameters are considered equal throughout the whole traffic network.

In this paper, we define $0 \leq \beta_i(t) \leq 1$ as the control command adjusting the suggested velocity to the vehicles. In particular, when $\beta_i(t) = 0$, the system is not controlled, and the macroscopic dynamics of the system follow the velocity-density steady-state behavior, which can be determined from the MFD. On the other hand, $\beta_i(t) = 1$ indicates that the controller is commanding the vehicles to stop.

The dynamics of a whole freeway traffic network consisting of n cells can be expressed as

$$\dot{x}(t) = f(x(t)) + G(x(t))u(t) + D(t) \quad (2a)$$

$$y(t) = Cx(t), \quad (2b)$$

where $t \geq 0$; $x(t) = [\rho_1(t) \dots \rho_n(t) v_1(t) \dots v_n(t)]^T \in \mathbb{R}^{2n}$ is the state vector, $y(t) = [\rho_s(t), \dots, \rho_m(t)]^T \in \mathbb{R}^{m-s+1}$ where $s \geq 2$ and $m \leq n$ is the output vector, $u(t) = [\beta_{s-1}(t) \dots \beta_m(t)]^T \in \mathbb{R}^{m-s+2}$ is the control input vector, $f(x(t)) = [\dot{\rho}_1(t) \dots \dot{\rho}_n(t) \hat{v}_1(t) \dots \hat{v}_n(t)]^T \in \mathbb{R}^{2n}$ where $\hat{v}_i(t) = \frac{1}{\tau} (V_i(t) - v_i(t)) + \frac{1}{L} [v_i(t) (v_{i-1}(t) - v_i(t)) - \frac{\varepsilon}{\tau} \frac{\rho_{i+1}(t) - \rho_i(t)}{\rho_i(t) + \kappa}]$, $G(x(t)) = \begin{bmatrix} [0]_{(m-s+2 \times n)} & [0]_{(m-s+2 \times s-2)} \\ [\hat{G}]_{(m-s+2 \times m-s+2)} & [0]_{(m-s+2 \times n-m)} \end{bmatrix}^T$ where $\hat{G} = \text{diag}\{-\frac{1}{\tau} V_{s-1}, \dots, -\frac{1}{\tau} V_m\}$ and, $D(t) = [D_1(t) \dots D_{2n}(t)]^T \in \mathbb{R}^{2n}$ is the unknown-and-unmeasured disturbance. The size of the control input vector $u(t)$ is larger because the control command is constrained ($0 \leq \beta(t) \leq 1$). Therefore, to control the density of the vehicle in cell \mathcal{C}_i , two control commands (two suggested velocities) shall be used (see the controllability matrix derived in [14]). These two control commands are the suggested velocity of the upstream cell \mathcal{C}_{i-1} and the suggested velocity of the target cell \mathcal{C}_i . By reducing the suggested velocity of the upstream cell, \mathcal{C}_{i-1} , the inflow to cell \mathcal{C}_i can be reduced. Also, by reducing the suggested velocity of the cell, \mathcal{C}_i , the outflow of cell \mathcal{C}_i can be reduced. Adjusting these two control commands, the density in cell \mathcal{C}_i can be increased or decreased.

III. HIERARCHICAL INFRASTRUCTURE-BASED CONTROLLER DESIGN

This section focuses on the design of a distributed hierarchical macroscopic traffic management controller to improve the performance of a homogeneous traffic network in terms of mobility, as shown in Fig. 2. The controller has a two-level structure with a D-ES controller at the upper level (shown in blue gradient color) and a D-FFL controller at the lower

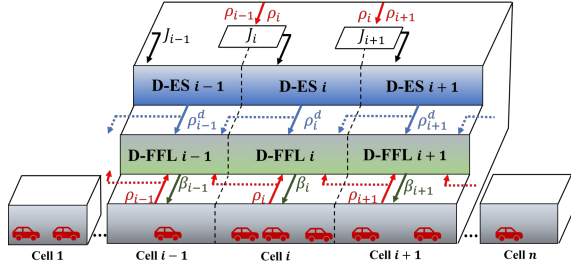


Fig. 2: Schematic of the whole traffic network with n cells consisting of the local hierarchical controller.

level (shown in green gradient color).

A. Lower-level Controller: D-FFL

At the lower level of the proposed hierarchical traffic control framework, we propose to employ a D-FFL controller to update the suggested velocity communicated to the vehicles so that the desired densities (determined by the D-ES in Section III.B) can be achieved. D-FFL relies on knowledge of the relative degree and the dynamic inversion matrix [12]. For a cell \mathcal{C}_i , the relative degree (\bar{q}) from u_i and u_{i-1} to y_i is 2. The D-FFL control design is based on the following assumptions.

Assumption 1: The disturbance $D(t)$ is continuous and $(\bar{q} - 1)$ -times differentiable.

Assumption 2: The reference model input $\rho^d(t)$ is bounded and \bar{q} -times differentiable.

Let us define the local reference model $\ddot{y}_m + \alpha_1 \dot{y}_m + \alpha_0 y_m = \ddot{\rho}^d + \zeta_1 \dot{\rho}^d + \zeta_0 \rho^d$, where ρ^d is the desired density of the target cell determined by the upper-level controller, and $\alpha_0, \alpha_1, \zeta_0, \zeta_1$ are constants. Also, let us define $e(t) = y(t) - y_m(t)$ as the error term and the square root of the average power of the density error as $\mathcal{P}_e = \left[\frac{1}{t_1 - t_0} \int_{t_0}^{t_1} e^T(\tau) e(\tau) d\tau \right]^{\frac{1}{2}}$. The control objective is to design a control input u that asymptotically stabilizes the closed-loop system and makes \mathcal{P}_e arbitrarily small. To this end, the ideal FL control input is given by [11]

$$u^d(x, \Phi_D, \Phi_r) = -M_u^{-\dagger} (M_u M_u^{-\dagger})^{-1} (\nu(x, \Phi_D, \Phi_r) + \Psi(x, \Phi_D)), \quad (3)$$

where $\Phi_r = [\rho^d \ \dot{\rho}^d \ \ddot{\rho}^d]^T$, $\Phi_D = [D \ \dot{D}]^T$, $\Psi(x, \Phi_D) = C \frac{\partial f}{\partial x}(f(x) + D) + CD$, and $\nu(x, \Phi_D, \Phi_r) = \ddot{\rho}^d + \zeta_1 \dot{\rho}^d + \zeta_0 \rho^d - \alpha_1 \dot{y}_m - \alpha_0 y_m$. Additionally, $M_u^{-\dagger}$ is the pseudo inverse of the dynamic inversion matrix M_u . Moreover, $M_u = C \frac{\partial f(x(t))}{\partial x} G(x(t))$ and for the traffic system defined in (2), we have

$$M_u = \begin{bmatrix} \rho_{s-1} V_{s-1} & -\rho_s V_s & 0 & \cdots & 0 \\ 0 & \rho_s V_s & -\rho_{s+1} V_{s+1} & \cdots & 0 \\ \vdots & \vdots & \ddots & \ddots & \vdots \\ 0 & \cdots & 0 & \rho_{m-1} V_{m-1} & -\rho_m V_m \end{bmatrix}. \quad (4)$$

Note that M_u is a non-square matrix. It can be shown that for the closed-loop system in (2)-(3), where $D = 0$ and

$u = u^d$, the zero dynamics is stable; therefore, the nonlinear closed-loop system is minimum phase.

The ideal control input u^d is not implementable because u^d depends on the measurement of the full state $x(t)$, knowledge of the uncertain dynamic function $f(x(t))$, and unknown disturbances $D(t)$. To address this issue, first, we assume that the FL control input u^d is sufficiently smooth, as stated in Assumption 3.

Assumption 3: For $i \in \mathcal{N}$, $\frac{\partial}{\partial x}[u_i^d(x, \Phi_D, \Phi_r)]$ and $\frac{\partial}{\partial \Phi_D}[u_i^d(x, \Phi_D, \Phi_r)]$ exist and are continuous.

Then, we generate the implementable control input u by passing u^d through the designed filter. Specifically,

$$[\mathbf{p}\bar{\sigma}_z(\mathbf{p})I + \sigma_z(0)M_u' M_u]u = \sigma_z(0)M_u' M_u u^d, \quad (5)$$

where $\mathbf{p} = d/dt$, M_u' is the transpose of M_u , $\sigma_z(s)$ is a monic polynomial with a degree $b \geq 2$ and real coefficients that are functions of a real parameter z . Thus, σ_z can be written as $\sigma_z = s^b + \sigma_{b-1,z}s^{b-1} + \cdots + \sigma_{1,z}s + \sigma_{0,z}$ where $\sigma_{0,z}, \cdots, \sigma_{b-1,z} \in \mathbb{R}$. The polynomial σ_z is a design parameter that must satisfy certain conditions listed in [15].

Combining (3) and (5) the FFL control input is

$$\mathbf{p}\bar{\sigma}_z(\mathbf{p})u = \sigma_z(0)M_u'[\ddot{\rho}^d + \zeta_1 \dot{\rho}^d + \zeta_0 \rho^d - \ddot{y} - \alpha_1 \dot{y} - \alpha_0 y]. \quad (6)$$

The controllers (3) and (6) are mathematically equivalent; however, unlike the FL control input (3), the FFL input in (6) does not require knowledge of $\Psi(x, \Phi_D)$ or the measurement of D and \dot{D} . The FFL control input is designed using the knowledge about the relative degree, the dynamic inversion matrix M_u , reference-model parameters $\alpha_1, \alpha_0, \zeta_1$ and ζ_0 and the filter polynomial ϱ_z , which depends on the real parameter z .

It should be noted that the arrays of M_u are functions of measured densities ρ_j , and V_j for $j \in \{s, \cdots, m\}$. Here, V_j , itself is a function of the free-flow velocity (v_{FF}), which is a predefined value and parameters a_m and $\rho_{c,j}$ (Please see Section II.) that may not be necessarily known. To address this issue, we define \bar{M}_u as an upper bound of M_u . In particular, since v_{FF} is an upper bound of V_j , we define \bar{M}_u to be

$$\bar{M}_u = \begin{bmatrix} \rho_{s-1} v_{FF} & -\rho_s v_{FF} & 0 & \cdots & 0 \\ 0 & \rho_s v_{s+1} & -\rho_{s+1} v_{FF} & \cdots & 0 \\ \vdots & \vdots & \ddots & \ddots & \vdots \\ 0 & \cdots & 0 & \rho_{m-1} v_{FF} & -\rho_m v_{FF} \end{bmatrix}. \quad (7)$$

Therefore, by replacing M_u with \bar{M}_u in (6), the FFL controller does not need to know the exact values of the state-dependent parameters in the METANET model.

Proposition 1: Consider the minimum phase system described by (2)-(6) under assumptions 1-3. For sufficiently large z value in the filter polynomial ϱ_z , the closed-loop (2)-(6) is asymptotically stable. The minimum stabilizing z depends on the system dynamics and its parameters.

Proof: The proof can be found in [11], [12].

Remark 1: The average power of the performance \mathcal{P}_e can be made arbitrarily small by a sufficiently large choice of z .

In practice, a nominal plant model can be used to determine a sufficiently large z that achieves stability and a

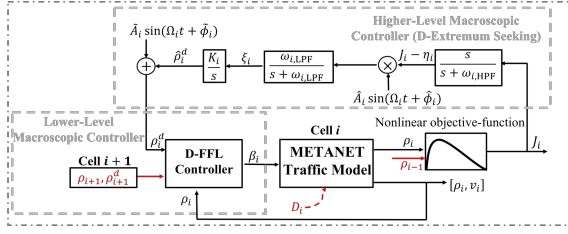


Fig. 3: Detailed schematic of the hierarchical controller design for cell i consisting of D-ES and D-FFL.

desired level of performance.

B. Higher-level Controller: D-ES

At the upper-level of the proposed hierarchical traffic control framework, we use a D-ES controller to determine an optimal density ρ^d within a congested cell \mathcal{C}_i . The goal is to maximize the average flow of the target cell to mitigate the traffic congestion while minimizing its flow difference with the upstream cell's flow to prevent back-propagating the congestion. In particular, for each congested cell, we define the following optimization problem

$$\max_{\rho_i} J_i(t) = w_{i,1}(t)Q_i^2(t) - w_{i,2}(t)[Q_i(t) - Q_{i-1}(t)]^2, \quad (8)$$

where $w_{i,1}(t)$ and $w_{i,2}(t)$ are the weights for each term in the cost function. In addition, $Q_i(t) = \rho_i(t)V_i(t)$ and it is subjected to the lower-level dynamics. Using (2) and (6), the lower-level dynamics are

$$\dot{X}_{LL} = \mathcal{F}_{LL}(X_{LL}, \mathcal{G}(X_{LL}, \rho^d)), \quad (9)$$

where $X_{LL} = [x \ u \ \dot{u} \ \dots \ u^{(b-1)}]$.

We designed a D-ES controller to solve the optimization problem in (8). Fig. 3 shows the details of the D-ES controller. The parameter that is optimized (ρ_i^d) is perturbed using a low-amplitude sinusoidal signal $\tilde{A}_i \sin(\Omega_i t + \tilde{\phi}_i)$. The perturbation frequency Ω_i must be chosen small enough to ensure that the lower-level dynamics appear as a static nonlinearity from the viewpoint of the ES loop [16]. Consider $\Omega_i = \mathcal{O}(\omega)$, $\omega_{i,HPF} = \mathcal{O}(\omega\Delta)$ and $\omega_{i,LPF} = \mathcal{O}(\omega\Delta)$ where \mathcal{O} is the statistic order, ω and Δ are small positive constants.

Remark 2: The convergence time of the desired density estimated by the ES is significantly slower than the response time of the inner loop, we can assume that the density reference is constant compared with the inner-loop dynamics.

Although increasing the perturbation frequency in gradient-based ES increases the convergence rate, the steady-state error will also increase significantly [16]. In this paper, we selected the perturbation frequency Ω_i to be 10 times slower than the lower-level dynamics. To ensure the stability and convergence of the D-ES controller, a set of assumptions shall be met [17].

Assumption 4: There exists a smooth function $\ell : \mathbb{R}^n \rightarrow \mathbb{R}^{m-s+1}$ such that $\mathcal{F}_{LL}(X_{LL}, \mathcal{G}(X_{LL}, \rho^d)) = 0$ if and only if $X_{LL} = \ell(\rho^d)$.

Assumption 5: For each $\rho^d \in \mathbb{R}^{m-s+1}$, the equilibrium $x = \ell(\rho^d)$ of the system $\dot{X}_{LL} = \mathcal{F}_{LL}(X_{LL}, \mathcal{G}(X_{LL}, \rho^d))$ is locally exponentially stable uniformly in ρ^d .

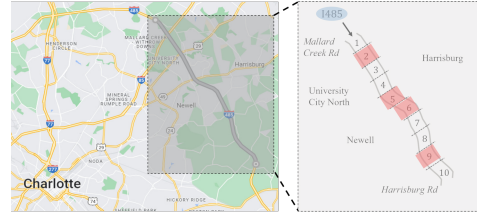


Fig. 4: 1485 inner highway between Mallard Creek Rd and Harrisburg Rd, Charlotte, North Carolina. Target cells 2, 5, 6, and 9 that are in the congested phase are highlighted.

Assumption 6: There exists $\rho^* \in \mathbb{R}^{m-s+1}$ such that $\frac{\partial}{\partial \rho^d} J(\rho^*) = 0$ and $\frac{\partial^2}{\partial \rho^d} J(\rho^*) < 0$.

In this paper, Assumptions 4 and 5 are met since the D-FFL controller guarantees the asymptotic stability of the lower-level dynamics (see Proposition 1). Finally, Assumption 6 is also met since the cost function in (8) is quadratic based on the form of the MFD function.

The following proposition summarizes the stability and convergence of the higher-level D-ES controller:

Proposition 2: Consider the closed-loop feedback system in Fig. 3 under Assumptions 4-6 with the control input (6). Recall that Remark 2 is in place. There exists $\bar{\omega} > 0$, and for any $\omega \in (0, \bar{\omega})$ there exists $\bar{\Delta}, \bar{A} > 0$ such that for the given ω and any $|\tilde{A}| \in (0, \bar{A})$ and $\Delta \in (0, \bar{\Delta})$ there exists a neighborhood of the point $(x, \rho^d, \xi, \eta) = (\ell(\rho^*), \rho^*, 0, J(\rho^*))$ such that any solution of the feedback system (2)-(6) from the neighborhood exponentially converges to an $\mathcal{O}(\omega + \Delta + |\tilde{A}|)$ -neighborhood of that point. Furthermore, $y(t)$ converges to an $\mathcal{O}(\omega + \Delta + |\tilde{A}|)$ -neighborhood of $J(\rho^*)$.

Proof: The proof can be found in [16], [17].

IV. SIMULATIONS & RESULTS

To demonstrate the effectiveness of the proposed hierarchical framework, we conduct a series of case studies. Fig. 4 is the schematic diagram of the freeway section used in these case studies. It is a subsection of I-485 inner highway, between Mallard Creek Rd and Harrisburg Rd, Charlotte, North Carolina. This section is approximately 10 miles long, with 4 lanes with a speed limit of 70 mph. We discretize this network into 10 cells, as shown in Fig. 4.

We adopt the model parameters of the METANET model to be $\varepsilon = 38 \frac{\text{mile}^2}{\text{h}}$, $\kappa = 18 \frac{\text{veh}}{\text{mile.h}}$, $\tau = 5s$, $\gamma = 4$, and $a_m = \mathfrak{h}(\rho_i)$, which is the only state-varying model parameter in this case study. In this research, we used brute-force search to find out the $\mathfrak{h}(\rho_i)$ function, which is equal to $[11, 7, 4, 1.5]$ if the density of the cell is $[\rho_i \leq \rho_c, \rho_c < \rho_i \leq 1.5\rho_c, 1.5\rho_c < \rho_i \leq 3\rho_c, 3\rho_c < \rho_i \leq \rho_J]$ respectively. Also, the critical density of the network is $\rho_c = 35 \frac{\text{veh}}{\text{mile.lane}}$, the jam density is $\rho_J = 150 \frac{\text{veh}}{\text{mile.lane}}$ and the free-flow velocity is $v_{FF} = 70$ mph. Furthermore, we select the origin flow as $q_0 = 1980$ veh/h. We selected these values by running PTV-VISSIM simulation using I-485 N of Exit 28 (Fig. 4) traffic flow data reported on Tuesday, 22 December 2020, at peak time between 4:30-5:30 PM and comparing the measured states with the homogeneous METANET model.

The flow disturbances in the traffic network are modeled as high amplitude low-frequency sine waves. Finally, the parameter values for each controller are listed here: $w_{i,1} = w_{i,2} = 1$ for $i \in \{2, 5, 6, 9\}$, $\hat{A}_i = \bar{A}_i = 1$, $\Omega_i = 0.001\pi \frac{\text{rad}}{\text{s}}$, $\omega_{i,\text{LPF}} = 0.5\Omega_i$, $\omega_{i,\text{HPF}} = 0.4\Omega_i$, $K_i = 1.35$ and $z = 1$.

A. Case-study 1: D-ES-FFL Performance

One of the common approaches in large network traffic control is to use a Proportional-Integral-Derivative (PID) feedback regulator for Mainstream Traffic Flow Control (MTFC) and use the VSL as an actuator [18]. In this case study, first, we compare the performance of the designed lower-level controller (D-FFL) with the PID-MTFC. To this end, a set point, which is typically the critical density value, is selected for cell 5. The proportional, integral, and derivative gains are $K_P = 11.2$, $K_I = 0.25$, and $K_D = 0.02$, respectively. The gains designed for the PID-MTFC approach were selected through numerical testing. These gains provide the best closed-loop command following for our problem. The density of the target cell 5 in both D-FFL and PID-MTFC scenarios is shown in Fig. 5. By comparing the results of the designed D-FFL controller and the PID-MTFC controller, it is found that D-FFL has a faster settling time. D-FFL is able to control the target cell to reach the desired density in 4 minutes, while it takes 9 minutes for PID-MTFC to reach the desired set-point. It should also be noted that in the proposed hierarchical control framework, the perturbation frequency of the higher-level controller (D-ES) depends on the time constant of the lower-level dynamics (lower-level controller + plant). Therefore, the overall convergence rate of the D-ES-FFL is faster than the ES-PID-MTFC controller.

Next, we present a numerical example showing the D-ES-FFL controller's effectiveness in mitigating congestion and preventing back-propagating congestion using the METANET model. This case study compares two scenarios where there is no active infrastructure controller in the traffic network versus when there is an active local D-ES-FFL controller for target cells in the traffic network. As shown in Fig. 4, the target cells 2, 5, 6, and 9 are on the verge of getting heavily congested due to the traffic network inflow and unknown downstream bottleneck.

In Fig. 6, the states of the target cells 5 and 6 and the upstream cell 4 are shown for both "D-ES-FFL" and "No-Control" scenarios. As shown, in the No-Control scenario,

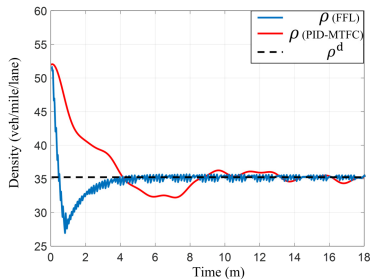


Fig. 5: Density changes of the target cell 5 using D-FFL controller (Blue) and PID-MTFC controller (Red).

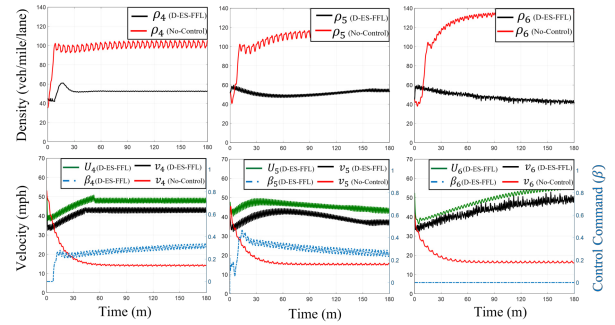


Fig. 6: States, Suggested velocities (solid green line) and control commands (dashed-dotted blue line) for cells 4, 5, and 6 in both scenarios.

the congestion starts back-propagating, and as the density increases, the congestion gets heavier, and the average velocity of each cell reduces. By activating the local "D-ES-FFL" controller, estimating the optimal densities of the cell, and finally tracking the optimal densities, the target cell avoids jam conditions. According to (8), the local objective function of each target cell is trying to maximize the average flow rate of the cell and minimize its flow difference with the upstream cell. In Fig. 7, the objective function values for cells 5 and 6 are shown in both scenarios. Furthermore, the total average flow of all cells upstream of the bottleneck ($Q_{\text{TOT}} = \sum_{i=1}^6 Q_i$) is shown. Finally, in Fig. 8, a colormap of the velocity changes in the whole network for the full-time spectrum is shown in both "No-Control" and "D-ES-FFL" scenarios.

B. Case-study 2: D-ES-FFL with PTV-VISSIM

In the second case study, we use a real-world traffic simulator, PTV Vissim, to show the effectiveness of D-ES-FFL control in a real-world traffic simulation with real-world traffic data. For this study, after the completion of each cycle (duration = 10 minutes), the density of the target cells is recorded and passed to the MATLAB-Simulink environment through the COM interface. Next, the local objective function of the congested cells is calculated and fed to the D-ES controller. Then, using the estimated optimal densities of D-ES in the Simulink, the suggested control commands are generated using the D-FFL controller. These commands are then passed to the MATLAB code and applied to the VISSIM through the COM interface to update the speed limit signs in the traffic network. We considered the same problem as case

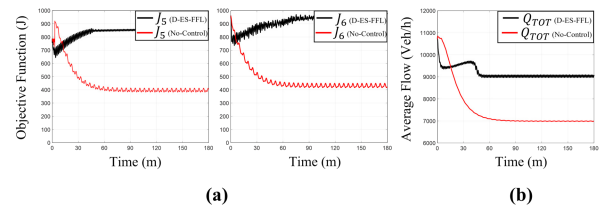


Fig. 7: Objective functions of target cells 5 and 6 (sub-plot a) and the total average flow of all cells upstream of the bottleneck (sub-plot b).

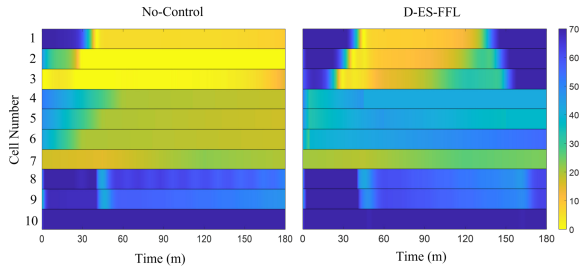


Fig. 8: Visualization of the traffic velocity data for the whole network in “No-Control” and “D-ES-FFL” scenarios.

study 1. The highway link has ten cells with freeway link behavior type, and each cell is 1 mile in length. The inflow on the traffic network was set equal to 1980 veh/h with the stochastic volume type. The vehicle class of the vehicles in the traffic network was chosen to be “Car” with the driving behavior of “Freeway”. To have a distributed traffic control network, we put the variable speed limit signs every 0.2 mile, so all vehicles in each cell get the suggested velocities information from the controller almost simultaneously. Also, in the first 12 minutes of the simulation, there is no active controller and effective communication between MATLAB and PTV VISSIM, so the desired initial conditions are reached. As it is shown in Fig. 9, by activating the “D-

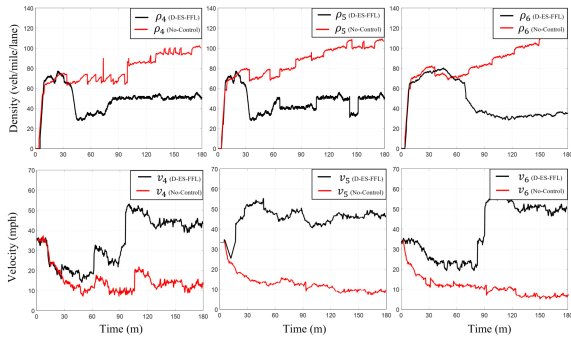


Fig. 9: States (density and velocity) cells 4, 5 and, 6 are shown using PTV-VISSIM in both scenarios.

ES-FFL” controller, the average velocity in target cells is greater than the “No-Control” scenario while its density is less congested.

V. CONCLUSIONS & FUTURE WORKS

This paper focuses on modeling and controlling a congested traffic network with multiple bottlenecks. We designed a hierarchical infrastructure-based controller to mitigate the traffic network’s congestion despite the unknown disturbances in the system. At the upper level, a Distributed Extremum Seeking (D-ES) controller aims to find the optimal operating densities of the target cell. At the lower level, a Distributed Filtered Feedback Linearization (D-FFL) controller tracks the desired density inputs from the higher level by controlling the suggested velocity of the vehicles in the target cell and its upstream cell. In the future, we will extend this case study to a traffic network consisting of

multiple classes of vehicles, such as Human-driven Vehicles (HDVs) and Autonomous Vehicles (AVs).

REFERENCES

- [1] Bob Pishue. Inrix global traffic scorecard—appendices. *INRIX research*, 2021.
- [2] Muhammad Sameer Sheikh and Yinqiao Peng. A comprehensive review on traffic control modeling for obtaining sustainable objectives in a freeway traffic environment. *Journal of Advanced Transportation*, 2022, 2022.
- [3] Mansour Johari, Mehdi Keyvan-Ekbatani, Ludovic Leclercq, Dong Ngoduy, and Hani S Mahmassani. Macroscopic network-level traffic models: Bridging fifty years of development toward the next era. *Transportation Research Part C: Emerging Technologies*, 131:103334, 2021.
- [4] Cédric Join, Hassane Abouaïssa, and Michel Fliess. Ramp metering: modeling, simulations and control issues. In *Advances in Distributed Parameter Systems*, pages 227–242. Springer, 2022.
- [5] Marcello Montanino, Julien Monteil, and Vincenzo Punzo. From homogeneous to heterogeneous traffic flows: Lp string stability under uncertain model parameters. *Transportation Research Part B: Methodological*, 146:136–154, 2021.
- [6] Apostolos Kotsialos, Markos Papageorgiou, Christina Diakaki, Yannis Pavlis, and Frans Middelham. Traffic flow modeling of large-scale motorway networks using the macroscopic modeling tool metanet. *IEEE Transactions on intelligent transportation systems*, 3(4):282–292, 2002.
- [7] Zejiang Wang, Xingyu Zhou, and Junmin Wang. Extremum-seeking-based adaptive model-free control and its application to automated vehicle path tracking. *IEEE/ASME Transactions on Mechatronics*, 2022.
- [8] Huan Yu, Jean Auriol, and Miroslav Krstic. Simultaneous downstream and upstream output-feedback stabilization of cascaded freeway traffic. *Automatica*, 136:110044, 2022.
- [9] Farzam Tajdari, Claudio Roncoli, Nikolaos Bekiaris-Liberis, and Markos Papageorgiou. Integrated ramp metering and lane-changing feedback control at motorway bottlenecks. In *2019 18th European Control Conference (ECC)*, pages 3179–3184. IEEE, 2019.
- [10] Qian Chen, Shihua Li, Chengchuan An, Jingxin Xia, and Wenming Rao. Feedback linearization-based perimeter controllers for oversaturated regions. *IEEE Intelligent Transportation Systems Magazine*, 14(1), 2022.
- [11] Jesse B Hoagg and TM Seigler. Filtered-dynamic-inversion control for unknown minimum-phase systems with unknown-and-unmeasured disturbances. *International Journal of Control*, 86(3):449–468, 2013.
- [12] AH Ghasemi, Jesse B Hoagg, and TM Seigler. Decentralized vibration and shape control of structures with colocated sensors and actuators. *Journal of Dynamic Systems, Measurement, and Control*, 138(3):031011, 2016.
- [13] Carlos F Daganzo and Nikolas Geroliminis. An analytical approximation for the macroscopic fundamental diagram of urban traffic. *Transportation Research Part B: Methodological*, 42(9):771–781, 2008.
- [14] Laura Muñoz, Xiaotian Sun, Roberto Horowitz, and Luis Alvarez. Traffic density estimation with the cell transmission model. In *Proceedings of the 2003 American Control Conference, 2003.*, volume 5, pages 3750–3755. IEEE, 2003.
- [15] Jesse B Hoagg and TM Seigler. Decentralized filtered dynamic inversion for uncertain minimum-phase systems. *Automatica*, 61:192–200, 2015.
- [16] Miroslav Krstić and Hsin-Hsiung Wang. Stability of extremum seeking feedback for general nonlinear dynamic systems. *Automatica*, 36(4):595–601, 2000.
- [17] Azad Ghaffari, Miroslav Krstić, and Sridhar Seshagiri. Power optimization for photovoltaic microconverters using multivariable newton-based extremum seeking. *IEEE Transactions on Control Systems Technology*, 22(6):2141–2149, 2014.
- [18] Rodrigo C Carlson, Ioannis Papamichail, Markos Papageorgiou, and Albert Messmer. Optimal mainstream traffic flow control of large-scale motorway networks. *Transportation Research Part C: Emerging Technologies*, 18(2):193–212, 2010.